

Increased Phonon Scattering by Nanograins and Point Defects in Nanostructured Silicon with a Low Concentration of Germanium

G. H. Zhu,¹ H. Lee,² Y. C. Lan,¹ X. W. Wang,¹ G. Joshi,¹ D. Z. Wang,¹ J. Yang,¹ D. Vashaee,³ H. Guilbert,¹ A. Pillitteri,¹ M. S. Dresselhaus,⁴ G. Chen,^{2,*} and Z. F. Ren^{1,*}

¹*Department of Physics, Boston College, Chestnut Hill, Massachusetts 02467, USA*

²*Department of Mechanical Engineering, Massachusetts Institute of Technology, Cambridge, Massachusetts 02139, USA*

³*Department of Electrical and Computer Engineering, Oklahoma State University, Tulsa, Oklahoma 74106, USA*

⁴*Department of Electrical Engineering and Computer Science, Massachusetts Institute of Technology, Cambridge, Massachusetts 02139, USA*

(Received 26 November 2008; published 14 May 2009)

The mechanism for phonon scattering by nanostructures and by point defects in nanostructured silicon (Si) and the silicon germanium (Ge) alloy and their thermoelectric properties are investigated. We found that the thermal conductivity is reduced by a factor of 10 in nanostructured Si in comparison with bulk crystalline Si. However, nanosize interfaces are not as effective as point defects in scattering phonons with wavelengths shorter than 1 nm. We further found that a 5 at. % Ge replacing Si is very efficient in scattering phonons shorter than 1 nm, resulting in a further thermal conductivity reduction by a factor of 2, thereby leading to a thermoelectric figure of merit 0.95 for Si₉₅Ge₅, similar to that of large grained Si₈₀Ge₂₀ alloys.

DOI: 10.1103/PhysRevLett.102.196803

PACS numbers: 73.50.Lw, 84.60.Rb, 85.80.Fi

Solid state energy conversion between heat and electricity based on thermoelectric effects is attractive in waste heat recovery and environmentally friendly refrigeration [1]. The conversion efficiency depends on the dimensionless thermoelectric figure of merit $ZT = (S^2\sigma/\kappa)T$, where S , σ , κ , and T are the Seebeck coefficient, electrical conductivity, thermal conductivity, and absolute temperature, respectively [1]. Good thermoelectric materials behave as crystals for electrons and glasses for phonons [2]. However, such materials are rare in nature and are not easily engineered in the laboratory. After the 1950s, ZT did not significantly improve for almost another 40 years. In the early 1990s, Hicks and Dresselhaus proposed the possibility to enhance ZT with nanostructures [3]. Recently, a number of studies reported high ZT values using nanostructures [4–8]. In these studies, the ZT enhancement in nanostructures was mostly due to their low thermal conductivity, which is attributed to phonon scattering by their large density of interfaces [9,10]. Among the various nanostructured materials, the nanostructured composite (nanocomposite) approach [7,8,10] seems to be the best.

For nanocomposites, when the grain size is smaller than the mean free path of a phonon, additional phonon scattering at boundaries will occur and the thermal conductivity is thereby reduced. The idea of reducing the thermal conductivity κ with smaller grains has been suggested since the 1980s [11], but most experimental efforts failed because the small grains also reduced the power factor $S^2\sigma$. Only recently, has a noticeable enhancement in ZT been achieved for the AgPbSbTe composite system [12], and for p -type BiSbTe [7,8], n -type Si₈₀Ge₂₀ [13] and p -type Si₈₀Ge₂₀ [14] systems. However, the reduction in κ from

the alloying comes through scattering by point defects, while for the nanosize effect it comes from the strong interface scattering of phonons. These two causes for phonon scattering could not be separated from one another in these studies. This distinction is the focus of the present Letter.

In focusing on the mechanisms of the reduction in the thermal conductivity in nanograined materials by comparison of the phonon scattering processes in pure Si and in Si containing a low Ge concentration, we note that pure Si does not have point defect scattering from Ge, and hence offers an opportunity to study the scattering of grain boundaries, while the addition of Ge increases point defect scattering. In the present work we find experimentally that nanograins play a very important role in increasing the phonon scattering for phonons with wavelengths in the nanometer range. However, point defect scattering, caused by alloying Ge into Si, is more effective in scattering phonons than just using pure Si nanostructures especially for scattering phonons with wavelengths of less than 1 nm. In the present work we show that a combination of nanograins and a 5 at. % Ge replacement of Si, that is Si₉₅Ge₅, produces both a reduction in the thermal conductivity and a similar ZT value to that of bulk Si₈₀Ge₂₀ alloys.

In our work, chunks of Si and Ge (Alfa Aesar), phosphorus (P) and gallium phosphide (GaP) (Sigma Aldrich) are pulverized into a powder until the desired nanosize particles are obtained [7,8,10,13,14]. P, a typical n -type dopant, introduced into our samples is 2.5 at. %, which is larger than the maximum bulk solubility limit of 1 at. %. With the addition of GaP and the introduction of nanosized particles, the solubility limit of P in Si or SiGe increases [15]. X-ray diffraction (XRD), scanning electron micros-

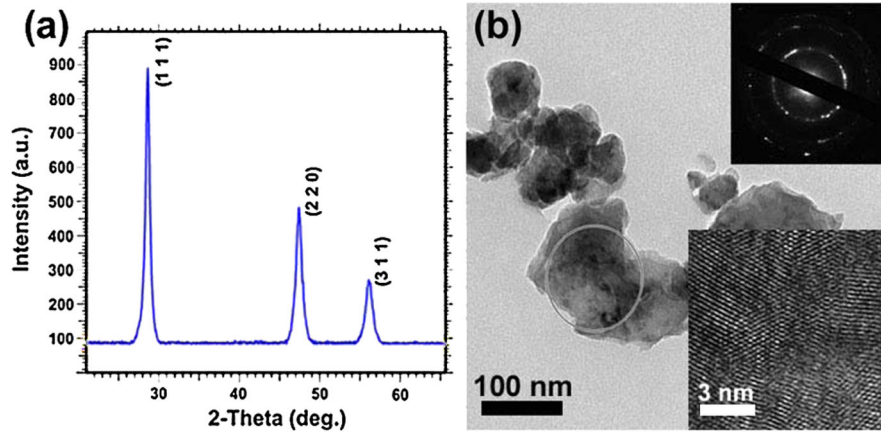


FIG. 1 (color online). XRD pattern (a), TEM image of ball milled $\text{Si}_{95}\text{Ge}_5$ nanopowders (b). The insets to Fig. 1 (b) are the diffraction pattern and HRTEM image for the circled region.

copy (SEM), and high resolution transmission electron microscopy (HRTEM) are used to characterize the structures of the samples. The nanopowder is pressed into disc specimens with a diameter of 12.7 mm and a thickness of a few mm by a quick dc hot press process [7,8,10,13,14]. The density of the hot pressed sample is measured using an Archimedes' kit and the value is very close to the theoretical density [16]. The thermal conductivity is measured using a laser flash system (Netzsch LFA457), and the electrical conductivity and Seebeck coefficient are measured simultaneously in a multiprobe transport system (Ulvac ZEM-3). The carrier concentration is measured using the van der Pauw method [17].

Figure 1(a) shows the XRD spectrum of our $\text{Si}_{95}\text{Ge}_5\text{P}_{2.5}(\text{GaP})_{1.5}$ nanopowders. It shows that the nanopowders have a single phase with broadened peaks indicating the nanosize of the grains in the range of 5–20 nm as obtained by the Williamson-Hall method [18]. Figure 1(b) shows the TEM image of the nanopowders around 20–150 nm, representing the size of the agglomeration of many smaller crystallites, indicated in the diffraction pattern [upper inset in Fig. 1(b)]. The HRTEM image [lower

inset in Fig. 1(b)] confirms the small size of the constituent particles.

Figure 2 shows the TEM images for the $\text{Si}_{95}\text{Ge}_5\text{P}_{2.5}(\text{GaP})_{1.5}$ sample after hot press, where most of the nanoparticles are in the 10–30 nm range, larger than the 5–20 nm initial nanoparticle range due to some grain growth during the hot press process. The HRTEM image [Fig. 2(b)] shows that the nanoparticles are highly crystallized and randomly oriented after hot press.

Figures 3(a)–3(f) show the comparative thermoelectric property measurement results for nanostructured Si, nanostructured $\text{Si}_{95}\text{Ge}_5$, bulk Si, and bulk $\text{Si}_{80}\text{Ge}_{20}$ alloy (RTG) that has been used by NASA for many years. Results plotted for the bulk Si are calculations using the Boltzmann transport equation within the relaxation time approximation, modified on the basis of the Vining model [19] but also considering nonparabolicity and a temperature-dependent band structure. Both the nanostructured Si and nanostructured $\text{Si}_{95}\text{Ge}_5$ samples show a higher electrical conductivity [Fig. 3(a)] but a lower absolute Seebeck coefficient [Fig. 3(b)] than that of the bulk $\text{Si}_{80}\text{Ge}_{20}$ RTG sample. This is mainly attributed to the

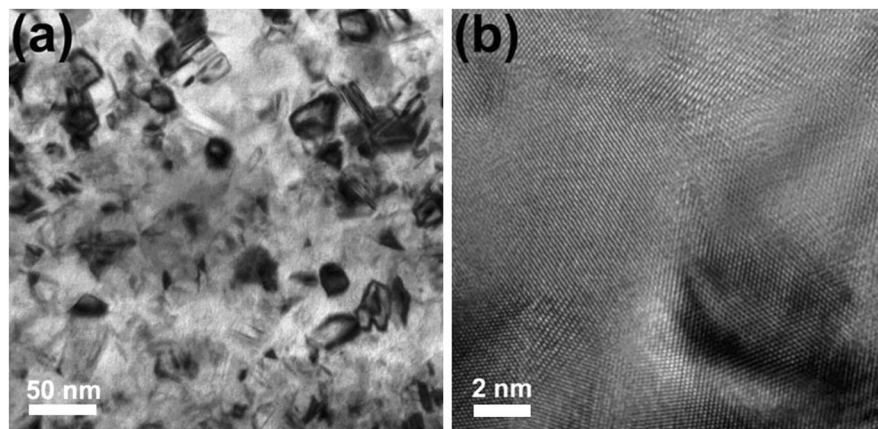


FIG. 2. Low (a) and high (b) magnification TEM images of the hot pressed nanostructured $\text{Si}_{95}\text{Ge}_5$ sample.

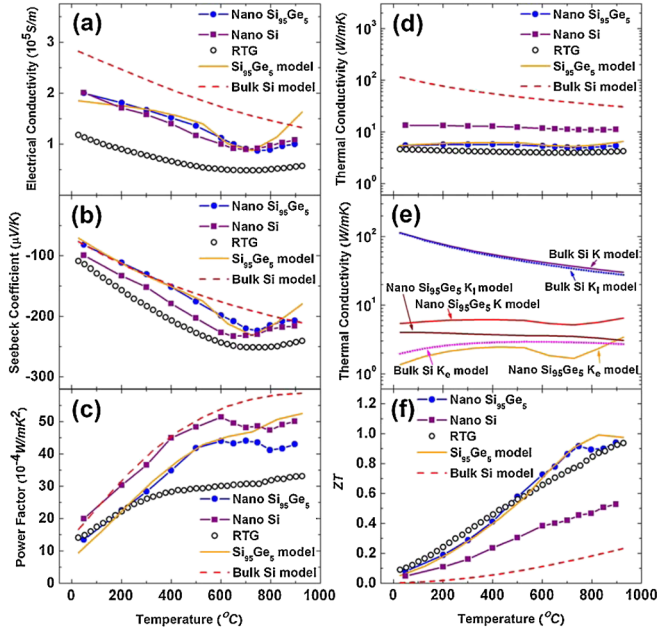


FIG. 3 (color online). Temperature-dependent electrical conductivity (a), Seebeck coefficient (b), power factor (c), thermal conductivity (d), electron (K_e), phonon (K_l), and total (K) thermal conductivity by modeling (e), and ZT (f) of nanostructured Si (filled squares), nanostructured $\text{Si}_{95}\text{Ge}_5$ (filled circles for experiment and solid line for model), bulk Si model (dashed line), and $\text{Si}_{80}\text{Ge}_{20}$ RTG samples (open circles).

higher solubility limit of P and the lower alloy scattering of charge carriers in nanostructured Si and nanostructured $\text{Si}_{95}\text{Ge}_5$ samples in comparison with the bulk $\text{Si}_{80}\text{Ge}_{20}$ RTG sample. The power factors for both nanostructured samples [Fig. 3(c)] are slightly lower than the values calculated for bulk materials with the same carrier concentration values as measured for the nanostructured samples. Also, due to the heavy doping in the nanostructured $\text{Si}_{95}\text{Ge}_5$ and Si samples and the activation of excess dopant (P) at high temperature during the measurement process, our nanostructured Si and nanostructured $\text{Si}_{95}\text{Ge}_5$ samples show different trends for the temperature-dependent electrical conductivity and Seebeck coefficient from those of the bulk Si. In fact, the power factor of the nanostructured $\text{Si}_{95}\text{Ge}_5$ sample is much higher than that of the bulk $\text{Si}_{80}\text{Ge}_{20}$ RTG sample [Fig. 3(c)], especially at temperatures above 300 °C.

The main advantage of the nanostructure approach for $\text{Si}_{95}\text{Ge}_5$ is that we can maintain the high electrical conductivity and power factor as shown in Figs. 3(a) and 3(c) and, at the same time, we can reduce the phonon thermal conductivity significantly. Such joint behavior does not occur in bulk samples. Figure 3(d) shows the temperature-dependent thermal conductivity of the nanostructured Si and nanostructured $\text{Si}_{95}\text{Ge}_5$ samples in comparison with bulk Si and bulk $\text{Si}_{80}\text{Ge}_{20}$ RTG samples. The thermal conductivity of the nanostructured Si shows a significant reduction (by about a factor of 10) compared with that of the heavily doped bulk Si, which is around

100 W/m · K at room temperature, a clear demonstration of the nanosize effect on phonon scattering. Moreover, with a 5 at. % replacement of Si by Ge, the thermal conductivity value of the nanostructured $\text{Si}_{95}\text{Ge}_5$ is even lower, close to that of the bulk $\text{Si}_{80}\text{Ge}_{20}$ RTG sample, caused by both the nanosize and point defect scattering effects in nanostructured $\text{Si}_{95}\text{Ge}_5$. Since the bulk $\text{Si}_{80}\text{Ge}_{20}$ RTG sample has 20 at. % Ge, and our nano $\text{Si}_{95}\text{Ge}_5$ sample has only 5 at. % Ge, a weaker alloy phonon scattering effect is expected in $\text{Si}_{95}\text{Ge}_5$. When the Ge concentration is increased from 5 to 20 at. %, the thermal conductivity is decreased by another factor of 2 to about 2–3 W/m · K, but the power factor is also decreased [13] accordingly because of the reduced charge mobility due to the alloy scattering of charge carriers.

The thermal conductivity of nanostructured $\text{Si}_{95}\text{Ge}_5$ has also been investigated by modeling based on Callaway's model [20] in combination with a modified effective medium theory [21] to consider the effect of nanosized grains. Figure 4(a) shows the mean free path of phonons vs phonon wavelength. For bulk Si, only three-phonon scattering and electron-phonon scattering are the dominant scattering mechanisms. As a 5 at. % of Ge is added, the scattering rate increases significantly due to point defect scattering. For pure Si, the mean free paths for most of the phonons will be limited by the small grain size. For $\text{Si}_{95}\text{Ge}_5$, the small grain size significantly reduces the mean free path of phonons at long wavelengths. Figure 4(b) shows the accumulative thermal conductivity normalized to the thermal conductivity of bulk Si as the phonon wavelength is increased. The thermal conductivity of pure Si is reduced almost by an order of magnitude using nanograins, since a 20 nm grain can reduce the mean free path of phonons at almost all wavelengths. By adding a 5 at. % Ge, alloy scattering can reduce the thermal conductivity more significantly than using nanograins in Si. As shown in Fig. 4(a), the mean free path by alloy scattering is even smaller than the grain size (20 nm) for phonon wavelengths less than 1 nm, and the contribution of short wavelength phonons is large. Nanosized grains in $\text{Si}_{95}\text{Ge}_5$ can further reduce the thermal conductivity by limiting the mean free path of phonons with wavelengths larger than 1 nm. As

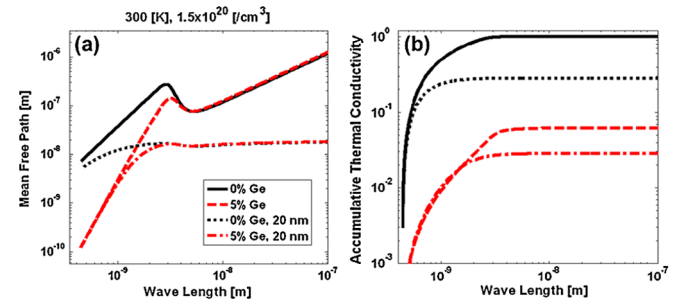


FIG. 4 (color online). Modeling results for the thermal conductivity at room temperature: (a) mean free path vs phonon wavelength and (b) accumulative thermal conductivity ratio vs phonon wavelength for different Ge ratios and grain sizes.

shown in Fig. 4(b), the thermal conductivity of nano-grained $\text{Si}_{95}\text{Ge}_5$ is reduced by a factor of 2 from bulk $\text{Si}_{95}\text{Ge}_5$. Thus, by using the nanostructures and also adding only a small amount of Ge, the thermal conductivity can be reduced to as low a value as for a SiGe alloy with a much higher Ge ratio.

Figure 3(e) shows that the calculated thermal conductivity of nanostructured $\text{Si}_{95}\text{Ge}_5$ matches well with the experimental results [Fig. 3(d)]. The electron contribution to the thermal conductivity is calculated from the electrical conductivity measurement results using the Wiedemann-Franz Law. The Lorenz number is calculated from the bulk model. Our modeling results show that the Lorenz number in bulk SiGe alloy varies from 1.3 to 2.2 from 25 °C to 1000 °C, and that variation within any specific temperature is 0.2 for the range of the doping concentration in our samples. The calculated phonon thermal conductivity dropped below 4 W/m · K at room temperature and reached ~ 3 W/m · K at 900 °C [Fig. 3(e)]. The low thermal conductivity for the nanostructured $\text{Si}_{95}\text{Ge}_5$ system is mainly attributed to both the enhanced boundary phonon scattering and the alloy effect. Thus, due to the significant thermal conductivity reduction without reducing the power factor, ZT of the nanostructured $\text{Si}_{95}\text{Ge}_5$ shows a maximum value of 0.95 at 900 °C, which is about the same as that of the bulk $\text{Si}_{80}\text{Ge}_{20}$ RTG sample [Fig. 3(f)].

While phonon scattering at the grain boundary can be explained by a modified effective medium theory, electron scattering due to a grain boundary with nanosize particles has not yet been well investigated. Our measurement results show that the electrical conductivity is slightly lower than the value expected for the given carrier concentration. There may be different explanations for the additional carrier scattering caused by grain boundaries, but the most plausible reason might be the electron potential variation at the grain boundaries due to defect sites and/or dopant precipitation at boundaries. Since our doping concentration is higher than the solubility limit, excess amount of dopants must be precipitated somewhere. A previous study suggested that P is likely to form a compound such as SiP which precipitates at the grain boundary [22]. Since the composition is different between the grain boundary region and the grain region, an electron potential difference will occur. These two effects can also happen in bulk Si, but the effect is greater in nanostructured $\text{Si}_{95}\text{Ge}_5$ due to a higher boundary density.

In summary, we have achieved an enhancement in ZT by a factor of 2 in nanostructured Si and of almost a factor of 4 in nanostructured $\text{Si}_{95}\text{Ge}_5$ in comparison with bulk Si. The enhancement is mainly due to the reduction in the thermal conductivity by the increased scattering of intermediate wavelength phonons at the nanosized grains and by the point defect scattering of short wavelength phonons. It is clearly demonstrated that phonons with different wavelengths need to be matched with similar size scatterers so that effective phonon scattering can take place to achieve the lowest possible thermal conductivity.

We would like to thank Drs. Jean-Pierre Fleurial and Pawan Gogna for providing the data for the RTG sample. The work was sponsored by DE-FG02-08ER46516 (M. D., G. C., and Z. F. R.), NSF NIRT 0506830 (M. D., G. C., and Z. F. R.), DOE DE-FG02-00ER45805 (Z. F. R.), and NSF CMMI 0833084 (Z. F. R. and G. C.).

*To whom correspondence should be addressed.

gchen2@mit.edu (G. C.); renzh@bc.edu (Z. F. R.)

- [1] C. Wood, Rep. Prog. Phys. **51**, 459 (1988).
- [2] G. Slack, in *CRC Handbook of Thermoelectrics*, edited by D. M. Rowe (CRC Press, Boca Raton, FL 1996).
- [3] L. D. Hicks and M. S. Dresselhaus, Phys. Rev. B **47**, 16 631 (1993).
- [4] R. Venkatasubramanian, E. Siivola, T. Colpitts, and B. O'Quinn, Nature (London) **413**, 597 (2001).
- [5] T. C. Harman, P. J. Taylor, M. P. Walsh, and B. E. LaForge, Science **303**, 818 (2004).
- [6] A. I. Hochbaum, R. Chen, R. D. Delgado, W. Liang, E. C. Garnett, M. Najarian, A. Majumdar, and P. D. Yang, Nature (London) **451**, 163 (2008); A. I. Boukai, Y. Bunimovich, J. Tahir-Kheli, J. Yu, W. A. Goddard, and J. R. Heath, Nature (London) **451**, 168 (2008).
- [7] B. Poudel, Q. Hao, Y. Ma, Y. C. Lan, A. Minnich, B. Yu, X. Yan, D. Z. Wang, A. Muto, D. Vashaee, X. Chen, J. M. Liu, M. S. Dresselhaus, G. Chen, and Z. F. Ren, Science **320**, 634 (2008).
- [8] Y. Ma, Q. Hao, B. Poudel, Y. C. Lan, B. Yu, D. Z. Wang, G. Chen, and Z. F. Ren, Nano Lett. **8**, 2580 (2008).
- [9] R. G. Yang and G. Chen, Phys. Rev. B **69**, 195316 (2004).
- [10] M. S. Dresselhaus, G. Chen, Z. F. Ren, J. P. Fleurial, and P. Gogna, Adv. Mater. **19**, 1043 (2007).
- [11] N. Savvides and H. J. Goldsmid, J. Phys. C **13**, 4671 (1980).
- [12] F. K. Hsu, S. Loo, F. Guo, W. Chen, J. S. Dyck, C. Uher, T. Hogan, E. K. Polychroniadis, and M. G. Kanatzidis, Science **303**, 818 (2004).
- [13] X. W. Wang, H. Lee, Y. C. Lan, G. H. Zhu, G. Joshi, D. Z. Wang, J. Yang, A. J. Muto, M. Y. Tang, J. Klatsky, S. Song, M. S. Dresselhaus, G. Chen, and Z. F. Ren, Appl. Phys. Lett. **93**, 193121 (2008).
- [14] G. Joshi, H. Lee, Y. C. Lan, X. W. Wang, G. H. Zhu, D. Z. Wang, A. J. Muto, M. Y. Tang, M. S. Dresselhaus, G. Chen, and Z. F. Ren, Nano Lett. **8**, 4670 (2008).
- [15] O. Yamashita, J. Appl. Phys. **89**, 6241 (2001).
- [16] J. P. Dismukes, L. Ekstrom, and R. J. Paff, J. Phys. Chem. **68**, 3021 (1964).
- [17] C. Wood, A. Lockwood, A. Chmielewski, J. Parker, and A. Zoltan, Rev. Sci. Instrum. **55**, 110 (1984).
- [18] G. K. Williamson and W. H. Hall, Acta Metall. **1**, 22 (1953).
- [19] C. B. Vining, J. Appl. Phys. **69**, 331 (1991).
- [20] J. Callaway and H. C. von Baeyer, Phys. Rev. **120**, 1149 (1960).
- [21] A. Minnich and G. Chen, Appl. Phys. Lett. **91**, 073105 (2007).
- [22] B. A. Cook, J. L. Haringa, S. H. Han, and C. B. Vining, J. Appl. Phys. **78**, 5474 (1995).